 CMC, vol.11, no.2, pp.79-107, 2009

Analytical Full-field Solutions of a Piezoelectric Layered Half-plane Subjected to Generalized Loadings

Chien-Ching Ma[1,2] **and Wen-Cha Wu**[2]

Abstract: The two-dimensional problem of a planar transversely isotropic piezoelectric layered half-plane subjected to generalized line forces and edge dislocations in the layer is analyzed by using the Fourier-transform method and the series expansion technique. The full-field solutions for displacements, stresses, electrical displacements and electric fields are expressed in explicit closed forms. The complete solutions consist only of the simplest solutions for an infinite piezoelectric medium with applied loadings. It is shown in this study that the physical meaning of this solution is the image method. The explicit solutions include Green's function for originally applied loadings in an infinite piezoelectric medium and the remaining terms are image singularities which are induced to satisfy free surface and interface continuity conditions. The mathematical method used in this study provides an automatic determination for the locations and magnitudes of all image singularities. The locations and magnitudes of image singularities are dependent on the piezoelectric material constants of the layered half-plane and the location of the applied loading. With the aid of the generalized Peach-Koehler formula, the image forces acting on dislocations are derived from the full-field solutions of the generalized stresses. Numerical results for the full-field distributions of stresses and electric fields in the piezoelectric layered half-plane and image forces for edge dislocations are presented based on the available analytical solutions.

Keywords: Piezoelectric material; Layered half-plane; Fourier transformation; Image method; Edge dislocation; Image force

1 Introduction

For a two-dimensional planar problem, the applied loadings are usually considered in two different types, concentrated forces and edge dislocations. In many appli-

[1] Corresponding author. Tel.: +886-2-23659996; Fax: +886-2-23631755; E-mail: ccma@ntu.edu.tw

[2] Department of Mechanical Engineering, National Taiwan University, Taipei, Taiwan 10617, Republic of China

cations, the elastic field due to loadings applied in the interior of the material is dislocations, the defect in the material. In order to understand the motion of a dislocation in an elastic material, one needs to calculate the stress distribution induced by the dislocation. For homogeneous elastic material in an unbounded medium, the elastic field around dislocations or concentrated loadings is generally well known. In most engineering applications, the geometrical configurations are all with finite boundary. Thus, the analysis of elastic field for material with finite boundary is necessary. Because of the complexity for the problem with finite boundary, there are few analytical results available in the literature. On the other hand, the layered half-plane subjected to surface tractions or body forces has very wide applications in a number of engineering fields. For example, the coating of a thin layer to protect soft matrices under contact and friction is a particular case of the problem. Furthermore, a wide range of electronic components are now manufactured by depositing semiconducting layers on supporting substrates.

Piezoelectric materials, which are coupled among the elastic and electric fields, have drawn considerable attentions in recent years. These materials can exchange energy from one form to the other and have been drawn considerable attentions for their promise potential in various applications such as transducer and sensors due to the coupling effect between mechanical and electric fields. In most of the applications, the laminated structures are widely used because of geometrical configurations all have finite boundaries. Thus, the analysis of piezoelectric material with a finite boundary is necessary. Furthermore, this material is generally brittle and defects (such as dislocations and cracks) may occur either during manufacturing processes or during service by the mechanical or electrical loadings. In other words, dislocations are the important defects that can adversely influence the performance of electronic devices. Therefore, to develop our understanding of the characteristics of these devices, a detailed knowledge of the behavior for piezoelectric materials subjected to loadings and dislocations is needed. It is also important to investigate the force exerted on dislocations due to the free surface, interface, the applied loadings and other defects. Solutions for the stresses induced by applied loadings and dislocations can be used to provide a direct means of determining the generalized Peach-Koehler (or image) force, which is of direct relevance in understanding the characteristics of the behavior for real dislocations.

The image method is a technique that uses a simple fundamental solution in an infinite plane to construct the solution for other more complicated boundary value problems. The use of the image method in solving two-dimensional isotropic problems dealing with screw dislocations for isotropic elastic material is well known and has been used successfully for simple cases of multilayered structures. The concept of semireflection and semitransmission mirrors was used to determine

the magnitudes and locations of the image screw dislocations without solving the boundary value problem. The multiple image problem for screw dislocations then becomes a combinatorial problem of counting reflections and transmissions for a given image path length. It was found that an infinite number of image screw dislocations were required. Basically, one can extend this methodology to include any number of layers, but as the number of layers increases, obtaining an explicit solution becomes extremely laborious and time consuming. By using the Fourier transform technique and a series expansion, an effective analytical methodology was developed by Lin and Ma (2000) to construct explicit analytical solutions for an anisotropic multilayered medium with n layers (the thickness in each layer is different) due to a screw dislocation in an arbitrary layer. The mathematical approach proposed by Lin and Ma (2000) is indeed the image method which provids an automatic determination for the magnitudes and locations of all the image screw dislocations.

For anisotropic elastic solids, the two-dimensional plane problems can be solved by a superposition of simple image singularities over the plane (Ting, 1996). The solution for a line dislocation in an infinite anisotropic medium has been obtained by Eshelby et al. (1953), Stroh (1958), and Willis (1970). Green's function for two-dimensional deformations of an anisotropic elastic half-space subjected to a line force and/or a line dislocation inside the half-space has been considered by Barnett and Lothe (1974), and Ting and Barnett (1993). The image singularities for isotropic elastic half-plane and bimaterials were discussed in detail by Ma and Lin (2001, 2002). Recently, theoretical analysis of screw dislocations and image forces in anisotropic multilayered media were presented by Ma and Lu (2006). For piezoelectric materials with electromechanical coupling, Green's functions have also been investigated by many authors. Pak (1990) considered a screw dislocation in an unbounded piezoelectric medium and derived the generalized Peach-Koehler forces acting on a screw dislocation subjected to external loads. The solution obtained was then used to derive the image fields for a half-space with traction free boundary. Based on the extended Stroh formulism, Green's functions were presented for the problem of defects interacting with a line dislocation in two-dimensional infinite anisotropic piezoelectric medium by Huang and Kuang (2001) and Chen et al. (2004). The interaction of defects and screw dislocations under antiplane mechanical and in-plane electrical loading in piezoelectric bimaterials was studied by Wu et al. (2003), Liu and Wang (2004), and Wang and Sudak (2007). The expressions for the image force acting on the screw dislocation due to its interaction were also derived. By using the Fourier-transform method, the full-field solution for the two-dimensional in-plane problem of piezoelectric bimaterials subjected to generalized loadings was obtained by Ma et al. (2008). The

number and distributed locations of image singularities were discussed in detail by Ma et al. (2008). Analytical solutions of a magnetoelectroelastic layered half-plane subjected to generalized anti-plane concentrated forces and screw dislocations were presented by Lee and Ma (2007). The solution obtained was then used to derive image forces of screw dislocations by Ma and Lee (2007). Wu et al. (2008) presented an overview of various three-dimensional analytical approaches for the analysis of multilayered and functionally graded piezoelectric plates and shells. Chen et al. (2009) solved antiplane piezoelectricity problems with multiple inclusions using the regularized meshless method.

The two-dimensional in-plane problem of a transversely isotropic piezoelectric layered half-plane subjected to generalized line forces and edge dislocations applied in the layer is analyzed in the present paper. By using the Fourier-transform method and the series expansion technique, an effective analytical methodology is developed in this study to construct theoretical solutions for this problem. The full-field analytical solutions for displacements, stresses, electrical displacements and electric fields are expressed in explicit closed-forms. The complete solutions consist only of the simplest solutions for an infinite piezoelectric medium with line loadings and edge dislocations. Except Green's functions for the originally applied singularities in an infinite medium, the remaining terms are image singularities which are induced to satisfy the free surface and interface continuity conditions. The physical meaning of the solutions can be regarded as the image method for the planar piezoelectric layered half-plane problem. The method of image is a technique that uses the superposition of known solution to construct the solution to other problems. However, only relatively simple problems, i.e., the half-plane and bimaterial, are presented in the literature. This study provides a methodology to construct the solution and it turns out to be the mathematical derivation of the image method for more complicated problem with finite boundaries. The locations and magnitudes of image singularities are determined automatically from this mathematic method. It is noted that the locations of image singularities are dependent on the material constants, the thickness of the layer and the location of the applied loadings. Base on the full-field solutions of the stresses and the generalized Peach-Koehler equation, the expressions of image forces exerted on edge dislocations can be obtained. For numerical examples, the full-field distributions of stresses, electric fields in the piezoelectric layered half-plane and image forces on edge dislocations are presented.

2 Basic Governing Equations and General Solutions in the Fourier-transform Domain

2.1 Governing equations for piezoelectric materials

In the absence of body force and electric charge density, the equilibrium equations for stresses and the Gauss's laws for electrostatics are given as

$$\sigma_{ij,j} = 0, \quad D_{i,i} = 0, \tag{1}$$

where σ_{ij} and D_i denote the stress tensor and electrical displacements, respectively. Here, repeated indices imply summation and a subscript comma stands for differentiation. For a linearly piezoelectric solid, the coupled constitutive relations are

$$\varepsilon_{ij} = S_{ijkl}\sigma_{kl} + \delta_{kij}D_k, \quad E_i = -\delta_{ikl}\sigma_{kl} - \beta_{ik}D_k \tag{2}$$

where ε_{ij} and E_i denote the strain tensor and electric fields, respectively. The material properties s_{ijkl}, β_{ik} and g_{kij} are the elastic compliance, dielectric impermeability, and piezoelectric constants, respectively. The strains and electric fields can be derived from the gradient of elastic displacements u_i and electric potential ϕ as follows

$$\varepsilon_{ij} = \frac{1}{2}(u_{i,j} + u_{j,i}), \quad E_i = -\phi_{,i}. \tag{3}$$

We consider a transversely isotropic piezoelectric material for the poling direction along the z direction. In such case, constitutive equations (2) can be simplified and are represented as the following matrix formulation:

$$\begin{bmatrix} \varepsilon_{xx} \\ \varepsilon_{yy} \\ \varepsilon_{zz} \\ 2\varepsilon_{yz} \\ 2\varepsilon_{xz} \\ 2\varepsilon_{xy} \end{bmatrix} = \begin{bmatrix} s_{11} & s_{12} & s_{13} & 0 & 0 & 0 \\ s_{12} & s_{11} & s_{13} & 0 & 0 & 0 \\ s_{13} & s_{13} & s_{33} & 0 & 0 & 0 \\ 0 & 0 & 0 & s_{44} & 0 & 0 \\ 0 & 0 & 0 & 0 & s_{44} & 0 \\ 0 & 0 & 0 & 0 & 0 & 2(s_{11}-s_{12}) \end{bmatrix} \begin{bmatrix} \sigma_{xx} \\ \sigma_{yy} \\ \sigma_{zz} \\ \sigma_{yz} \\ \sigma_{xz} \\ \sigma_{xy} \end{bmatrix} + \begin{bmatrix} 0 & 0 & g_{31} \\ 0 & 0 & g_{31} \\ 0 & 0 & g_{33} \\ 0 & g_{15} & 0 \\ g_{15} & 0 & 0 \\ 0 & 0 & 0 \end{bmatrix} \begin{bmatrix} D_x \\ D_y \\ D_z \end{bmatrix},$$

$$\begin{bmatrix} E_x \\ E_y \\ E_z \end{bmatrix} = - \begin{bmatrix} 0 & 0 & 0 & 0 & g_{15} & 0 \\ 0 & 0 & 0 & g_{15} & 0 & 0 \\ g_{31} & g_{31} & g_{33} & 0 & 0 & 0 \end{bmatrix} \begin{bmatrix} \sigma_{xx} \\ \sigma_{yy} \\ \sigma_{zz} \\ \sigma_{yz} \\ \sigma_{xz} \\ \sigma_{xy} \end{bmatrix} + \begin{bmatrix} \beta_{11} & 0 & 0 \\ 0 & \beta_{11} & 0 \\ 0 & 0 & \beta_{33} \end{bmatrix} \begin{bmatrix} D_x \\ D_y \\ D_z \end{bmatrix}. \tag{4}$$

For the two-dimensional in-plane problem of piezoelectric materials, the body is assumed to be plane deformation and subjected to plane electric fields. In this case, the isotropic plane is assumed to be perpendicular to the z-axis in the Cartesian coordinate system. When the x-z plane is defined as the deformation plane, the elastic displacements $u_x(x,z)$ and $u_z(x,z)$, and electric potential $\phi(x,z)$ are functions of x and z only. Since the elastic displacement in the y direction is zero, i.e., $u_y = 0$, the generalized plane strain conditions give $\varepsilon_{yy} = E_y = 0$. The two-dimensional constitutive equations for this planar problem can be simplified as

$$\begin{bmatrix} \varepsilon_{xx} \\ \varepsilon_{zz} \\ 2\varepsilon_{xz} \\ E_x \\ E_z \end{bmatrix} = \begin{bmatrix} a_{11} & a_{12} & 0 & 0 & b_{21} \\ a_{12} & a_{22} & 0 & 0 & b_{22} \\ 0 & 0 & a_{33} & b_{13} & 0 \\ 0 & 0 & -b_{13} & d_{11} & 0 \\ -b_{21} & -b_{22} & 0 & 0 & d_{22} \end{bmatrix} \begin{bmatrix} \sigma_{xx} \\ \sigma_{zz} \\ \sigma_{xz} \\ D_x \\ D_z \end{bmatrix}, \tag{5}$$

where

$$a_{11} = s_{11} - \frac{s_{12}^2}{s_{11}}, \quad a_{12} = s_{13} - \frac{s_{12}s_{13}}{s_{11}}, \quad a_{22} = s_{33} - \frac{s_{13}^2}{s_{11}}, \quad a_{33} = s_{44},$$

$$b_{13} = g_{15}, \quad b_{21} = \left(1 - \frac{s_{12}}{s_{11}}\right) g_{31}, \quad b_{22} = g_{33} - \frac{s_{13}}{s_{11}} g_{31},$$

$$d_{11} = \beta_{11}, \quad d_{22} = \beta_{33} + \frac{g_{31}^2}{s_{11}}.$$

In the absence of body force and electric charge density, the equilibrium equations can be expressed as

$$\frac{\partial \sigma_{xx}}{\partial x} + \frac{\partial \sigma_{xz}}{\partial z} = 0, \quad \frac{\partial \sigma_{xz}}{\partial x} + \frac{\partial \sigma_{zz}}{\partial z} = 0, \quad \frac{\partial D_x}{\partial x} + \frac{\partial D_z}{\partial z} = 0. \tag{6}$$

Furthermore, the compatibility relations for strains and electric fields are given by

$$\frac{\partial^2 \varepsilon_{xx}}{\partial z^2} + \frac{\partial^2 \varepsilon_{zz}}{\partial x^2} - 2\frac{\partial^2 \varepsilon_{xz}}{\partial x \partial z} = 0, \quad \frac{\partial E_x}{\partial z} - \frac{\partial E_z}{\partial x} = 0. \tag{7}$$

In order to satisfy the equilibrium equations, the stresses and electrical displacements are represented by the stress function $\chi(x,z)$ and the electrical displacement function $\varphi(x,z)$, respectively, as follows

$$\begin{aligned} &\sigma_{xx} = \frac{\partial^2 \chi}{\partial z^2}, \ \sigma_{xz} = -\frac{\partial^2 \chi}{\partial x \partial z}, \ \sigma_{zz} = \frac{\partial^2 \chi}{\partial x^2}, \\ &D_x = \frac{\partial \varphi}{\partial z}, \ D_z = -\frac{\partial \varphi}{\partial x}. \end{aligned} \tag{8}$$

Substituting Eqs. (8) and (5) into the compatibility equation (7) leads to two coupled homogeneous partial differential equations for $\chi(x,z)$ and $\varphi(x,z)$

$$\left[a_{22}\frac{\partial^4}{\partial x^4}+(2a_{12}+a_{33})\frac{\partial^4}{\partial x^2\partial z^2}+a_{11}\frac{\partial^4}{\partial z^4}\right]\chi - \left[(b_{21}+b_{13})\frac{\partial^3}{\partial x\partial z^2}+b_{22}\frac{\partial^3}{\partial x^3}\right]\varphi=0,$$

$$\left[(b_{13}+b_{21})\frac{\partial^3}{\partial x\partial z^2}+b_{22}\frac{\partial^3}{\partial x^3}\right]\chi+\left(d_{11}\frac{\partial^2}{\partial z^2}+d_{22}\frac{\partial^2}{\partial x^2}\right)\varphi=0. \tag{9}$$

By eliminating φ in Eq. (9), we can obtain a homogeneous partial differential equation of sixth order for the stress function $\chi(x,z)$ as follow

$$\left(\kappa_4\frac{\partial^6}{\partial x^6}+\kappa_3\frac{\partial^6}{\partial x^4\partial z^2}+\kappa_2\frac{\partial^6}{\partial x^2\partial z^4}+\kappa_1\frac{\partial^6}{\partial z^6}\right)\chi=0, \tag{10}$$

where

$$\begin{aligned}&\kappa_1=a_{11}d_{11},\ \kappa_2=2a_{12}d_{11}+a_{33}d_{11}+a_{11}d_{22}+b_{21}^2+b_{13}^2+2b_{21}b_{13},\\&\kappa_3=a_{22}d_{11}+2a_{12}d_{22}+a_{33}d_{22}+2b_{22}b_{21}+2b_{13}b_{22},\ \kappa_4=a_{22}d_{22}+b_{22}^2.\end{aligned} \tag{11}$$

Fourier-transform with respect to the spatial coordinate x with parameter ω is applied to solve the partial differential equation (i.e., Eq. (10)). Take the Fourier-transform pairs of the stress function $\chi(x,z)$, defines as

$$\tilde{\chi}(\omega,z)=\int_{-\infty}^{\infty}\chi(x,z)e^{-i\omega x}dx,\quad \chi(x,z)=\frac{1}{2\pi}\int_{-\infty}^{\infty}\tilde{\chi}(\omega,z)e^{i\omega x}d\omega. \tag{12}$$

Then, Eq. (10) is simplified to an ordinary differential equation for$\tilde{\chi}(\omega,z)$,

$$\left(\kappa_1\frac{\partial^6}{\partial z^6}-\kappa_2\omega^2\frac{\partial^4}{\partial z^4}+\kappa_3\omega^4\frac{\partial^6}{\partial z^2}-\kappa_4\omega^6\right)\tilde{\chi}=0. \tag{13}$$

The general solution of Eq. (13) is expressed as

$$\tilde{\chi}(\omega,z)=\sum_{k=1}^{6}C_k e^{i\omega p_k z}, \tag{14}$$

where C_k are undetermined coefficients and p_k $(k=1\sim 6)$ are the roots of the following characteristic equation (Rajapakse, 1997; Sosa, 1991) which depend on the piezoelectric material constants

$$\kappa_1 p^6+\kappa_2 p^4+\kappa_3 p^2+\kappa_4=0. \tag{15}$$

In addition, the same equation (15) can be applied for $\tilde{\varphi}$, hence $\tilde{\chi}$ and $\tilde{\varphi}$ have the similar solution form.

2.2 Properties of roots for the characteristic equation

For the particular material symmetry property of the piezoelectric material, the characteristic equation (15) is expressed in terms of even powers of p and is a polynomial of degree three for p^2. If the three roots of p^2 are assumed to be m_i $(i = 1 \sim 3)$, the characteristic equation can be rewritten as

$$\kappa_1 m^3 + \kappa_2 m^2 + \kappa_3 m + \kappa_4 = 0. \tag{16}$$

Therefore, the roots m_i can be expressed explicitly as (Ma et al., 2008)

$$\begin{aligned} m_1 &= S + T - \frac{1}{3}\frac{\kappa_2}{\kappa_1}, \\ m_{2,3} &= -\frac{1}{2}(S+T) - \frac{1}{3}\frac{\kappa_2}{\kappa_1} \pm \frac{i}{2}\sqrt{3}(S-T), \end{aligned} \tag{17}$$

where

$$\begin{aligned} Q &= \frac{\kappa_3}{3\kappa_1} - \left(\frac{\kappa_2}{3\kappa_1}\right)^2, \\ R &= \frac{\kappa_2\kappa_3}{6\kappa_1^2} - \frac{\kappa_4}{2\kappa_1} - \left(\frac{\kappa_2}{3\kappa_1}\right)^3, \\ S &= \sqrt[3]{R + \sqrt{Q^3 + R^2}}, \quad T = \sqrt[3]{R - \sqrt{Q^3 + R^2}}. \end{aligned} \tag{18}$$

Since the cubic equation in Eq. (16) has different real coefficients, there have no identical characteristic root in piezoelectric materials (i.e., discriminating factor $\Delta(= Q^3 + R^2) = 0$). Besides, the characteristic equation cannot have any real roots if the generalized strain energy is positive. It can be shown that the six roots of the characteristic equation consist of three distinct complex conjugate pairs. If p_k $(k = 1 \sim 6)$ are the roots, we let

$$p_k = \alpha_k + i\beta_k, \quad p_{k+3} = \bar{p}_k, \quad k = 1 \sim 3, \tag{19}$$

where α_k and β_k are real, with $\beta_k > 0$. In general, there are two possible cases for p and will be presented below. Case (1), if the discriminating factor is negative (i.e., $\Delta < 0$), all of the three roots in p^2 must be negative real. We then have

$$p_1 = i\beta_1, \quad p_2 = i\beta_2, \quad p_3 = i\beta_3, \tag{20}$$

where β_1, β_2, and β_3 are real and positive, with $\beta_j > \beta_{j+1}$, $j = 1 \sim 2$. Case (2), only one roots of p^2, say p_1^2 is real, and the other two roots p_2^2 and p_3^2 must be complex conjugates (i.e., $\Delta > 0$). We have

$$p_1 = i\beta_1, \quad p_2 = \alpha + i\beta_2, \quad p_3 = -\alpha + i\beta_2, \tag{21}$$

in which α is real, and β_1, and β_2 are real and positive.

2.3 The general solutions for field quantities

In this study, the piezoelectric layered half-plane is considered in which two piezoelectric materials are involved. From Eq. (14), the general solutions of displacements, stresses, electric potential, electrical displacements and electric fields in the Fourier-transform domain can be obtained as follows (Ma et al., 2008)

$$\tilde{u}_x^{(j)}(\omega,z) = i\omega \sum_{k=1}^{6} \xi_k^{(j)} C_k^{(j)} e^{i\omega p_k^{(j)} z}, \quad \tilde{u}_z^{(j)}(\omega,z) = i\omega \sum_{k=1}^{6} \eta_k^{(j)} C_k^{(j)} e^{i\omega p_k^{(j)} z},$$

$$\tilde{\sigma}_{xx}^{(j)}(\omega,z) = -\omega^2 \sum_{k=1}^{6} (p_k^{(j)})^2 C_k^{(j)} e^{i\omega p_k^{(j)} z}, \quad \tilde{\sigma}_{xz}^{(j)}(\omega,z) = \omega^2 \sum_{k=1}^{6} p_k^{(j)} C_k^{(j)} e^{i\omega p_k^{(j)} z},$$

$$\tilde{\sigma}_{zz}^{(j)}(\omega,z) = -\omega^2 \sum_{k=1}^{6} C_k^{(j)} e^{i\omega p_k^{(j)} z}, \quad \tilde{\phi}^{(j)}(\omega,z) = i\omega \sum_{k=1}^{6} \varsigma_k^{(j)} C_k^{(j)} e^{i\omega p_k^{(j)} z}, \tag{22}$$

$$\tilde{E}_x^{(j)}(\omega,z) = \omega^2 \sum_{k=1}^{6} \varsigma_k^{(j)} C_k^{(j)} e^{i\omega p_k^{(j)} z}, \quad \tilde{E}_z^{(j)}(\omega,z) = \omega^2 \sum_{k=1}^{6} \gamma_k^{(j)} p_k^{(j)} C_k^{(j)} e^{i\omega p_k^{(j)} z},$$

$$\tilde{D}_x^{(j)}(\omega,z) = \omega^2 \sum_{k=1}^{6} \lambda_k^{(j)} p_k^{(j)} C_k^{(j)} e^{i\omega p_k^{(j)} z}, \quad \tilde{D}_z^{(j)}(\omega,z) = -\omega^2 \sum_{k=1}^{6} \lambda_k^{(j)} C_k^{(j)} e^{i\omega p_k^{(j)} z},$$

where

$$\xi_k^{(j)} = a_{11}^{(j)} (p_k^{(j)})^2 + a_{12}^{(j)} + b_{21}^{(j)} \lambda_k^{(j)}, \quad \eta_k^{(j)} = \left[a_{12}^{(j)} (p_k^{(j)})^2 + a_{22}^{(j)} + b_{22}^{(j)} \lambda_k^{(j)} \right] \Big/ p_k^{(j)},$$

$$\varsigma_k^{(j)} = \left(-b_{13}^{(j)} + d_{11}^{(j)} \lambda_k^{(j)} \right) p_k^{(j)}, \quad \gamma_k^{(j)} = b_{21}^{(j)} (p_k^{(j)})^2 + b_{22}^{(j)} - d_{22}^{(j)} \lambda_k^{(j)},$$

$$\lambda_k^{(j)} = \left[b_{22}^{(j)} + \left(b_{31}^{(j)} + b_{21}^{(j)} \right) \left(p_k^{(j)} \right)^2 \right] / \left[d_{11}^{(j)} \left(p_k^{(j)} \right)^2 + d_{22}^{(j)} \right]. \tag{23}$$

In Eqs. (22) and (23), the superscripts (j) denote the quantities associated with the material j (i.e.,j=1, 2). The undetermined coefficients $C_k^{(j)}$ can be obtained by applying the jump, boundary and continuity conditions for the piezoelectric layered half-plane. According to the conjugate property for characteristic root p, it is interesting to note that there exist conjugate relations for Eq. (23), i.e., $\xi_{k+3}^{(j)} = \bar{\xi}_k^{(j)}$, $\eta_{k+3}^{(j)} = \bar{\eta}_k^{(j)}$, $\varsigma_{k+3}^{(j)} = \bar{\varsigma}_k^{(j)}$, $\gamma_{k+3}^{(j)} = \bar{\gamma}_k^{(j)}$, $\lambda_{k+3}^{(j)} = \bar{\lambda}_k^{(j)}$.

3 Explicit Full-field Solutions for Piezoelectric Layered Half-plane

Consider a two-dimensional piezoelectroic layered half-plane with a straight perfectly bonded interface at z=0 as shown in Fig. 1. Let material 1 and material 2 be occupied by the thin layer $(0 \leq z \leq h)$ with thickness h and the half-plane $(-\infty < z \leq 0)$, respectively. A generalized line force **f** (i.e., line forces f_x and f_z, a line electric charge Q) and a generalized line dislocation **b** (i.e., edge dislocations b_x and b_z, an electric-potential dislocation b_ϕ) are applied at $(x,\, z) = (0,\, d)$ with $h \geq d \geq 0$, which is in the thin layer (i.e., material 1). Without loss of generality, we take the plane $z = d$, $x < 0$ as the slip plane of the generalized dislocations. The jump conditions for applied generalized forces and dislocations at $(0,\, d)$ are expressed as

$$\left.\begin{bmatrix} \sigma_{zz}^{(1)} \\ \sigma_{xz}^{(1)} \\ u_x^{(1)} \\ u_z^{(1)} \\ D_z^{(1)} \\ \phi^{(1)} \end{bmatrix}\right|_{z=d^+} - \left.\begin{bmatrix} \sigma_{zz}^{(1)} \\ \sigma_{xz}^{(1)} \\ u_x^{(1)} \\ u_z^{(1)} \\ D_z^{(1)} \\ \phi^{(1)} \end{bmatrix}\right|_{z=d^-} = \begin{bmatrix} -f_z\delta(x) \\ -f_x\delta(x) \\ b_x H(x) \\ b_z H(x) \\ Q\delta(x) \\ b_\phi H(x) \end{bmatrix}.$$

The jump conditions in the Fourier transform domain are

$$\left.\begin{bmatrix} \tilde{\sigma}_{zz}^{(1)} \\ \tilde{\sigma}_{xz}^{(1)} \\ \tilde{u}_x^{(1)} \\ \tilde{u}_z^{(1)} \\ \tilde{D}_z^{(1)} \\ \tilde{\phi}^{(1)} \end{bmatrix}\right|_{z=d^+} - \left.\begin{bmatrix} \tilde{\sigma}_{zz}^{(1)} \\ \tilde{\sigma}_{xz}^{(1)} \\ \tilde{u}_x^{(1)} \\ \tilde{u}_z^{(1)} \\ \tilde{D}_z^{(1)} \\ \tilde{\phi}^{(1)} \end{bmatrix}\right|_{z=d^-} = \begin{bmatrix} -f_z \\ -f_x \\ \frac{1}{i\varphi} b_x \\ \frac{1}{i\omega} b_z \\ Q \\ \frac{1}{i\omega} b_\phi \end{bmatrix}. \tag{24}$$

From the general solutions presented in Eq. (22) and substituting Eq. (22) into Eq. (24), we have

$$\left[C_i^{(1+)}\right] - \left[C_i^{(1-)}\right] = \frac{1}{\omega^2} \left[F_{ij}^{(1)}\right]^{-1}\Big|_{z=d} [q_j], \tag{25}$$

where superscripts '–' and '+' indicate the undetermined coefficients $C_i^{(1)}$ for $0 \leq$

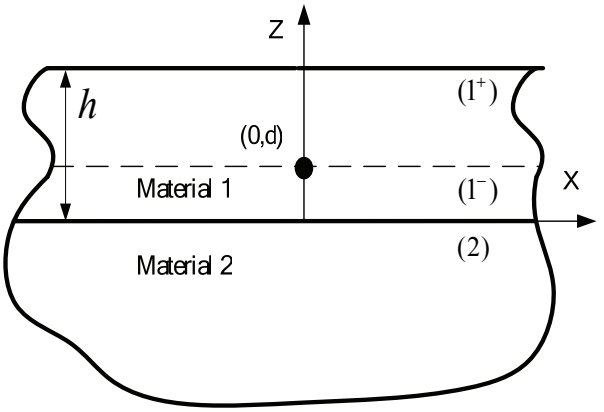

Figure 1: Configuration and coordinate system of a piezoelectric layered half-plane subjected to generalized loadings.

$z \le d$ and $d \le z \le h$, respectively, and $\left[F_{ij}^{(1)}\right]$ is a diagonal matrix,

$$\left[F_{ij}^{(1)}\right] = \begin{bmatrix} e^{i\omega p_1^{(1)} z} & 0 & 0 & 0 & 0 & 0 \\ 0 & e^{i\omega p_2^{(1)} z} & 0 & 0 & 0 & 0 \\ 0 & 0 & e^{i\omega p_3^{(1)} z} & 0 & 0 & 0 \\ 0 & 0 & 0 & e^{i\omega p_4^{(1)} z} & 0 & 0 \\ 0 & 0 & 0 & 0 & e^{i\omega p_5^{(1)} z} & 0 \\ 0 & 0 & 0 & 0 & 0 & e^{i\omega p_6^{(1)} z} \end{bmatrix}, \tag{26}$$

$$[q_j] = \left[\rho_{ij}^{(1)}\right]^{-1} \left[-f_z, -f_x, -\frac{1}{i\omega} b_x, -\frac{1}{i\omega} b_z, Q, \frac{1}{i\omega} b_\phi\right]^T, \tag{27}$$

$$\left[\rho_{ij}^{(1)}\right] = \begin{bmatrix} -1 & -1 & -1 & -1 & -1 & -1 \\ p_1^{(1)} & p_2^{(1)} & p_3^{(1)} & p_4^{(1)} & p_5^{(1)} & p_6^{(1)} \\ \frac{-1}{i\omega}\xi_1^{(1)} & \frac{-1}{i\omega}\xi_2^{(1)} & \frac{-1}{i\omega}\xi_3^{(1)} & \frac{-1}{i\omega}\xi_4^{(1)} & \frac{-1}{i\omega}\xi_5^{(1)} & \frac{-1}{i\omega}\xi_6^{(1)} \\ \frac{-1}{i\omega}\eta_1^{(1)} & \frac{-1}{i\omega}\eta_2^{(1)} & \frac{-1}{i\omega}\eta_3^{(1)} & \frac{-1}{i\omega}\eta_4^{(1)} & \frac{-1}{i\omega}\eta_5^{(1)} & \frac{-1}{i\omega}\eta_6^{(1)} \\ -\lambda_1^{(1)} & -\lambda_2^{(1)} & -\lambda_3^{(1)} & -\lambda_4^{(1)} & -\lambda_5^{(1)} & -\lambda_6^{(1)} \\ \frac{-1}{i\omega}\varsigma_1^{(1)} & \frac{-1}{i\omega}\varsigma_2^{(1)} & \frac{-1}{i\omega}\varsigma_3^{(1)} & \frac{-1}{i\omega}\varsigma_4^{(1)} & \frac{-1}{i\omega}\varsigma_5^{(1)} & \frac{-1}{i\omega}\varsigma_6^{(1)} \end{bmatrix}. \tag{28}$$

The boundary conditions on the top surface (i.e., z=h) of the thin layer can be

written as

$$\left[\begin{array}{c}\tilde{\sigma}_{zz}^{(1+)}\\ \tilde{\sigma}_{xz}^{(1+)}\\ \tilde{D}_{z}^{(1+)}\end{array}\right]\Bigg|_{z=h}=\omega^{2}\left[\begin{array}{cccccc}\rho_{11}^{(1)} & \rho_{12}^{(1)} & \rho_{13}^{(1)} & \rho_{14}^{(1)} & \rho_{15}^{(1)} & \rho_{16}^{(1)}\\ \rho_{21}^{(1)} & \rho_{22}^{(1)} & \rho_{23}^{(1)} & \rho_{24}^{(1)} & \rho_{25}^{(1)} & \rho_{26}^{(1)}\\ \rho_{51}^{(1)} & \rho_{52}^{(1)} & \rho_{53}^{(1)} & \rho_{54}^{(1)} & \rho_{55}^{(1)} & \rho_{56}^{(1)}\end{array}\right]\left[F_{ij}^{(1)}\right]\Big|_{z=h}\left[C_{i}^{(1+)}\right]=0. \tag{29}$$

The coefficients $C_i^{(1+)}$ are related as follows

$$\left[\begin{array}{c}C_{4}^{(1+)}\\ C_{5}^{(1+)}\\ C_{6}^{(1+)}\end{array}\right]=\left[\Omega_{ij}e^{i\omega\left(p_{j}^{(1)}-p_{i+3}^{(1)}\right)}\right]\left[\begin{array}{c}C_{1}^{(1+)}\\ C_{2}^{(1+)}\\ C_{3}^{(1+)}\end{array}\right], \tag{30}$$

where

$$[\Omega_{ij}]=-\left[\begin{array}{ccc}\rho_{14}^{(1)} & \rho_{15}^{(1)} & \rho_{16}^{(1)}\\ \rho_{24}^{(1)} & \rho_{25}^{(1)} & \rho_{26}^{(1)}\\ \rho_{54}^{(1)} & \rho_{55}^{(1)} & \rho_{56}^{(1)}\end{array}\right]^{-1}\left[\begin{array}{ccc}\rho_{11}^{(1)} & \rho_{12}^{(1)} & \rho_{13}^{(1)}\\ \rho_{21}^{(1)} & \rho_{22}^{(1)} & \rho_{23}^{(1)}\\ \rho_{51}^{(1)} & \rho_{52}^{(1)} & \rho_{53}^{(1)}\end{array}\right]. \tag{31}$$

The continuity conditions of the generalized stresses and displacements at the interface $z=0$ are

$$\left[\begin{array}{c}\tilde{\sigma}_{zz}^{(2)}\\ \tilde{\sigma}_{xz}^{(2)}\\ \tilde{u}_{x}^{(2)}\\ \tilde{u}_{z}^{(2)}\\ \tilde{D}_{z}^{(2)}\\ \tilde{\phi}^{(2)}\end{array}\right]\Bigg|_{z=0}=\left[\begin{array}{c}\tilde{\sigma}_{zz}^{(1-)}\\ \tilde{\sigma}_{xz}^{(1-)}\\ \tilde{u}_{x}^{(1-)}\\ \tilde{u}_{z}^{(1-)}\\ \tilde{D}_{z}^{(1-)}\\ \tilde{\phi}^{(1-)}\end{array}\right]\Bigg|_{z=0}. \tag{32}$$

We rewrite Eq. (32) in terms of $C_i^{(1-)}$ and $C_i^{(2)}$ as

$$\omega^{2}\left[\rho_{ij}^{(2)}\right]\left[C_{i}^{(2)}\right]-\omega^{2}\left[\rho_{ij}^{(1)}\right]\left[C_{i}^{(1-)}\right]=0,$$

or

$$\left[C_{i}^{(1-)}\right]=-\left[G_{ij}\right]\left[C_{j}^{(2)}\right], \tag{33}$$

where

$$[G_{ij}]=-\left[\rho_{ki}^{(1)}\right]^{-1}\left[\rho_{kj}^{(2)}\right]. \tag{34}$$

For $\omega > 0$, the bounded conditions of all physical quantities at infinity for the half-plane require that

$$C_1^{(2)} = C_2^{(2)} = C_3^{(2)} = 0. \tag{35}$$

We have the following relationship of the undetermined coefficients

$$\begin{bmatrix} 1 & 0 & 0 & G_{14} & G_{15} & G_{16} \\ 0 & 1 & 0 & G_{24} & G_{25} & G_{26} \\ 0 & 0 & 1 & G_{34} & G_{35} & G_{36} \\ \Omega_{11}e^{i\omega\left(p_1^{(1)}-p_4^{(1)}\right)h} & \Omega_{12}e^{i\omega\left(p_2^{(1)}-p_4^{(1)}\right)h} & \Omega_{13}e^{i\omega\left(p_3^{(1)}-p_4^{(1)}\right)h} & G_{44} & G_{45} & G_{46} \\ \Omega_{21}e^{i\omega\left(p_1^{(1)}-p_5^{(1)}\right)h} & \Omega_{22}e^{i\omega\left(p_2^{(1)}-p_5^{(1)}\right)h} & \Omega_{23}e^{i\omega\left(p_3^{(1)}-p_5^{(1)}\right)h} & G_{54} & G_{55} & G_{56} \\ \Omega_{31}e^{i\omega\left(p_1^{(1)}-p_6^{(1)}\right)h} & \Omega_{32}e^{i\omega\left(p_2^{(1)}-p_6^{(1)}\right)h} & \Omega_{33}e^{i\omega\left(p_3^{(1)}-p_6^{(1)}\right)h} & G_{64} & G_{65} & G_{66} \end{bmatrix}$$

$$\begin{bmatrix} C_1^{(1+)} \\ C_2^{(1+)} \\ C_3^{(1+)} \\ C_4^{(2)} \\ C_5^{(2)} \\ C_6^{(2)} \end{bmatrix} = \frac{1}{\omega^2} \begin{bmatrix} q_1 e^{-i\omega p_1^{(1)} d} \\ q_2 e^{-i\omega p_2^{(1)} d} \\ q_3 e^{-i\omega p_3^{(1)} d} \\ q_4 e^{-i\omega p_4^{(1)} d} \\ q_5 e^{-i\omega p_5^{(1)} d} \\ q_6 e^{-i\omega p_6^{(1)} d} \end{bmatrix}. \tag{36}$$

By omitting the lengthy algebraic derivation, the undetermined coefficients can be obtained as follows

$$\begin{bmatrix} C_1^{(1-)} \\ C_2^{(1-)} \\ C_3^{(1-)} \\ C_4^{(1-)} \\ C_5^{(1-)} \\ C_6^{(1-)} \end{bmatrix} = \frac{1}{\omega^2} \frac{1}{\det|U|} \begin{bmatrix} \sum_{l=4}^{6}\sum_{i=1}^{6}\sum_{j=1}^{6}\sum_{k=j+1}^{6} q_i\, z_{lijk} G_{1l}\, e^{i\omega\left(\left(p_i^{(1)}+p_j^{(1)}+p_k^{(1)}\right)h - p_i^{(1)}d\right)} \\ \sum_{l=4}^{6}\sum_{i=1}^{6}\sum_{j=1}^{6}\sum_{k=j+1}^{6} q_i\, z_{lijk} G_{2l}\, e^{i\omega\left(\left(p_i^{(1)}+p_j^{(1)}+p_k^{(1)}\right)h - p_i^{(1)}d\right)} \\ \sum_{l=4}^{6}\sum_{i=1}^{6}\sum_{j=1}^{6}\sum_{k=j+1}^{6} q_i\, z_{lijk} G_{3l}\, e^{i\omega\left(\left(p_i^{(1)}+p_j^{(1)}+p_k^{(1)}\right)h - p_i^{(1)}d\right)} \\ \sum_{l=4}^{6}\sum_{i=1}^{6}\sum_{j=1}^{6}\sum_{k=j+1}^{6} q_i\, z_{lijk} G_{4l}\, e^{i\omega\left(\left(p_i^{(1)}+p_j^{(1)}+p_k^{(1)}\right)h - p_i^{(1)}d\right)} \\ \sum_{l=4}^{6}\sum_{i=1}^{6}\sum_{j=1}^{6}\sum_{k=j+1}^{6} q_i\, z_{lijk} G_{5l}\, e^{i\omega\left(\left(p_i^{(1)}+p_j^{(1)}+p_k^{(1)}\right)h - p_i^{(1)}d\right)} \\ \sum_{l=4}^{6}\sum_{i=1}^{6}\sum_{j=1}^{6}\sum_{k=j+1}^{6} q_i\, z_{lijk} G_{6l}\, e^{i\omega\left(\left(p_i^{(1)}+p_j^{(1)}+p_k^{(1)}\right)h - p_i^{(1)}d\right)} \end{bmatrix}, \tag{37}$$

and

$$\begin{bmatrix} C_4^{(2)} \\ C_5^{(2)} \\ C_6^{(2)} \end{bmatrix} = \frac{1}{\omega^2}\frac{1}{\det|U|} \begin{bmatrix} \sum_{i=1}^{6}\sum_{j=1}^{6}\sum_{k=j+1}^{6} q_i\, z_{4ijk}\, e^{i\omega\left(\left(p_i^{(1)}+p_j^{(1)}+p_k^{(1)}\right)h-p_i^{(1)}d\right)} \\ \sum_{i=1}^{6}\sum_{j=1}^{6}\sum_{k=j+1}^{6} q_i\, z_{5ijk}\, e^{i\omega\left(\left(p_i^{(1)}+p_j^{(1)}+p_k^{(1)}\right)h-p_i^{(1)}d\right)} \\ \sum_{i=1}^{6}\sum_{j=1}^{6}\sum_{k=j+1}^{6} q_i\, z_{6ijk}\, e^{i\omega\left(\left(p_i^{(1)}+p_j^{(1)}+p_k^{(1)}\right)h-p_i^{(1)}d\right)} \end{bmatrix}, \tag{38}$$

where

$$\det|U| = \sum_{l=1}^{6}\sum_{m=l+1}^{6}\sum_{n=m+1}^{6} A_{lmn} e^{-i\omega\left(p_l^{(1)}+p_m^{(1)}+p_n^{(1)}\right)h}, \tag{39}$$

$$A_{ijk} = -\sum_{l=4}^{6}\sum_{m=4}^{6}\sum_{n=4}^{6} e'_{lmn} G_{(i+3)l} G_{(j+3)m} G_{(k+3)n}, \quad i=1 \;\; j=2 \;\; k=3$$

$$A_{ijk} = \frac{1}{2}\sum_{s=1}^{3}\sum_{l=4}^{6}\sum_{m=4}^{6}\sum_{n=4}^{6}\sum_{x=4}^{6}\sum_{y=4}^{6} e'_{kxy} e'_{lmn} e_{ijs} \Omega_{(k-3)s} G_{sl} G_{xm} G_{yn} (-1)^{i+j+1}, \quad i,j=1,2,3 \;\; k=4,5,6 \tag{40}$$

$$A_{ijk} = -\sum_{x=1}^{3}\sum_{y=1}^{3}\sum_{p=1}^{3}\sum_{t=1}^{3}\sum_{l=4}^{6}\sum_{m=4}^{6}\sum_{n=4}^{6}\sum_{r=4}^{6} e'_{lmn} e'_{jkr} e_{ipt} e_{ixy} \Omega_{(j-3)x} \Omega_{(k-3)y} G_{pl} G_{tm} G_{rn}, \quad i=1,2,3 \;\; j,k=4,5,6$$

$$A_{ijk} = -\sum_{l=1}^{3}\sum_{m=1}^{3}\sum_{n=1}^{3}\sum_{p=1}^{3}\sum_{q=1}^{3}\sum_{r=1}^{3} e_{lmn} e_{pqr} \Omega_{l1} \Omega_{m2} \Omega_{n3} G_{p4} G_{q5} G_{r6}, \quad i=4 \;\; j=5 \;\; k=6,$$

$$
\begin{aligned}
z_{sijk} &= \sum_{l=1}^{3}\sum_{m=1}^{3}\sum_{n=1}^{3}\sum_{x=4}^{6}\sum_{y=4}^{6} e'_{sxy}e_{lmn}G_{jx}G_{ky}\Omega_{1l}\Omega_{2m}\Omega_{3n}(-1)^{i}, \quad i,j,k=1,2,3\\
z_{sijk} &= \sum_{l=4}^{6}\sum_{m=4}^{6}\sum_{n=4}^{6}\sum_{x=4}^{6}\sum_{y=4}^{6} e'_{smn}e'_{lxy}G_{jx}G_{ky}\Omega_{(m-3)i}\Omega_{(n-3)j}, \quad i,j=1,2,3 \quad k=4,5,6\\
z_{sijk} &= -\sum_{l=4}^{6}\sum_{m=4}^{6}\sum_{x=4}^{6}\sum_{y=4}^{6} e'_{skm}e'_{lxy}G_{jx}G_{ky}\Omega_{(m-3)i}, \quad i=1,2,3 \quad j,k=4,5,6\\
z_{sijk} &= \sum_{m=4}^{6}\sum_{n=4}^{6}\sum_{x=4}^{6}\sum_{y=4}^{6} e'_{imn}e'_{sxy}G_{jx}G_{ky}\Omega_{(m-3)j}\Omega_{(n-3)k}, \quad i=4,5,6 \quad j,k=1,2,3\\
z_{sijk} &= -\sum_{m=4}^{6}\sum_{x=4}^{6}\sum_{y=4}^{6} e'_{ikm}e'_{sxy}G_{jx}G_{ky}\Omega_{(m-3)j}, \quad i,k=4,5,6 \quad j=1,2,3\\
z_{sijk} &= \sum_{x=4}^{6}\sum_{y=4}^{6} e'_{sxy}G_{jx}G_{ky}(-1)^{i}, \quad i,j,k=4,5,6
\end{aligned}
\tag{41}
$$

and $e_{123}=e_{231}=e_{312}=1$, $e_{321}=e_{213}=e_{132}=-1$, $e_{ijk}=0$if two or more subscript are equal, $e'_{456}=e'_{645}=e'_{564}=1$, $e'_{654}=e'_{546}=e'_{465}=-1$, $e'_{ijk}=0$ if two or more subscript are equal. Because the denominator in Eqs. (37) and (38) are so complicated that it is not possible to obtain the inverse Fourier transform directly. In order to obtain the explicit analytical full-field solutions from inverse Fourier transform, the denominator $\det|U|$ in Eqs. (37) and (38) should be reformulated. By examining the structure of $\det|U|$, the term with magnitude $A_{123}e^{-i\omega(p_1+p_2+p_3)h}$ is taken out from $\det|U|$ so that

$$
\det|U| = A_{123}e^{-i\omega(p_1+p_2+p_3)h}\left(1-\det|*|\right), \tag{42}
$$

where

$$
\det|*| = 1-\sum_{l=1}^{6}\sum_{m=l+1}^{6}\sum_{n=m+1}^{6}\frac{A_{lmn}}{A_{123}}e^{-i\omega(p_l+p_m+p_n-p_1-p_2-p_3)h}. \tag{43}
$$

It can be shown that $\det|*|<1$ for $\omega>0$. Hence, by expansion of $\frac{1}{\det|U|}$ into a

power series of $\det|*|$, we obtain

$$\begin{aligned}\frac{1}{\det|U|} &= \frac{e^{i\omega(p_1+p_2+p_3)h}}{A_{123}(1-\det|*|)} = \sum_{n=0}^{\infty}\frac{e^{i\omega(p_1+p_2+p_3)h}}{A_{123}}(\det|*|)^n \\ &= \sum_{n=0}^{\infty}\left(\frac{e^{i\omega(p_1+p_2+p_3)h}}{A_{123}}\right)^{n+1}\left(-\sum_{l=1}^{6}\sum_{m=l+1}^{6}\sum_{n=m+1}^{6}A_{lmn}e^{-i\omega(p_l+p_m+p_n)h}\right)^n \\ &= \sum_{n=0}^{\infty}\sum(-1)^n v\,A_{123}^{-(n+1)}\,\hat{A}\,e^{-i\omega\left(\hat{P}-(p_1+p_2+p_3)(n+1)\right)h},\end{aligned} \tag{44}$$

where

$$\sum = \sum_{n_1=0}^{n}\sum_{n_2=0}^{n-n_1}\sum_{n_3=0}^{n-n_1-n_2}\cdots\sum_{n_{12}=0}^{n-n_1-n_2\cdots-n_{11}},$$

$$n_1+n_2+\ldots+n_{13}=n, \quad v=\frac{n!}{n_1!\,n_2!\,n_3!\cdots n_{12}!\,n_{13}!},$$

and "!" represents factorial. As we have mentioned in the previous section that there are two possible cases for the characteristic root p. The expressions for $\hat{A}$ and $\hat{P}$ in Eq. (44) depend on the characteristic root p, and the results are presented as follows.

case 1 $p_1=i\beta_1$, $p_2=i\beta_2$, $p_3=i\beta_3$, $p_4=\bar{p}_1$, $p_5=\bar{p}_2$, $p_6=\bar{p}_3$

$$\begin{aligned}\hat{P} = &\sum_{i=1}^{6}p_i n_i + (p_1+p_2+p_6)(n_7-n_{11}) + (p_1+p_3+p_5)(n_8-n_{10}) \\ &+ (p_2+p_3+p_4)(n_9-n_{12}) + (p_4+p_5+p_6)n_{13},\end{aligned} \tag{45}$$

$$\begin{aligned}\hat{A} = &(A_{125}+A_{136})^{n_1}\ (A_{124}+A_{236})^{n_2}\ (A_{134}+A_{235})^{n_3}\ (A_{245}+A_{346})^{n_4} \\ &(A_{145}+A_{356})^{n_5}\ (A_{146}+A_{256})^{n_6} \\ &(A_{126})^{n_7}(A_{135})^{n_8}(A_{234})^{n_9}(A_{246})^{n_{10}}(A_{345})^{n_{11}}(A_{156})^{n_{12}}(A_{456})^{n_{13}}.\end{aligned} \tag{46}$$

case 2 $p_1=i\beta_1$, $p_2=\alpha+i\beta_2$, $p_3=-\alpha+i\beta_2$, $p_4=\bar{p}_1$, $p_5=\bar{p}_2$, $p_6=\bar{p}_3$

$$\begin{aligned}\hat{P} = &\sum_{i=1}^{6}p_i n_i + (p_1+p_2+p_5)(n_7-n_{11}) + (p_1+p_3+p_6)(n_8-n_{10}) \\ &+ (p_2+p_3+p_4)(n_9-n_{12}) + (p_4+p_5+p_6)n_{13},\end{aligned} \tag{47}$$

$$\hat{A} = (A_{126}+A_{135})^{n_1}\ (A_{124}+A_{235})^{n_2}\ (A_{134}+A_{236})^{n_3}\ (A_{246}+A_{345})^{n_4}$$
$$(A_{145}+A_{256})^{n_5}\ (A_{146}+A_{356})^{n_6} \tag{48}$$
$$(A_{125})^{n_7}(A_{136})^{n_8}(A_{234})^{n_9}(A_{245})^{n_{10}}(A_{346})^{n_{11}}(A_{156})^{n_{12}}(A_{456})^{n_{13}}.$$

By omitting the details of the derivation, the solutions for the unknown coefficients in Eqs. (37) and (38) can be expressed in explicit forms as follows

$$C_s^{(1-)} = \sum_{n=0}^{\infty}\sum\sum_{l=4}^{6}\sum_{i=1}^{6}\sum_{j=1}^{6}\sum_{k=j+1}^{6}(-1)^n v\, A_{123}^{-(n+1)}\hat{A}q_i z_{lijk}G_{sl}$$
$$e^{i\omega\left(\left(-\hat{P}+(p_1+p_2+p_3)(n+1)+p_i^{(1)}+p_j^{(1)}+p_k^{(1)}\right)h-p_i^{(1)}d\right)}, \tag{49}$$

$$C_s^{(2)} = \sum_{n=0}^{\infty}\sum\sum_{i=1}^{6}\sum_{j=1}^{6}\sum_{k=j+1}^{6}(-1)^n vA_{123}^{-(n+1)}\hat{A}q_i z_{sijk}$$
$$e^{i\omega\left(\left(-\hat{P}+(p_1+p_2+p_3)(n+1)+p_i^{(1)}+p_j^{(1)}+p_k^{(1)}\right)h-p_i^{(1)}d\right)}. \tag{50}$$

Now, the solutions are linear combinations of exponential functions, i.e., $\mathbf{M}e^{i\omega N}$; each term represents the Green's function in the transform domain for concentrated loadings in an infinite homogeneous medium. The term with N in the exponential functions indicates the location of the loading and $\mathbf{M}$ represents the magnitude of the loading. The location of the loading depends on the thickness of the thin layer h, the position of applied loadings d and eigenvalues p_j. The magnitude of $\mathbf{M}$ only depends on material constants. Since the solutions in the transformed domain expressed in Eq. (22) are exponential functions of ω, only the following inverse Fourier transformation is required, which is

$$\frac{1}{2\pi}\int_{-\infty}^{\infty} e^{i\omega(pz+H)}e^{i\omega x}d\omega = \frac{1}{\pi}Re\left[\frac{i}{x+pz+H}\right],$$

where H is an arbitrary constant. Therefore, the inverse Fourier transformation for Eq. (22) can be easily obtained term by term. Finally, the exact closed-form solutions of displacements, stresses, electrical displacements and electric fields for the piezoelectric layered half-plane are presented in very compact forms as follows:

$$\sigma_{xx}^{(1)} = -\frac{1}{\pi}Re\left(\sum_{k=1}^{6}\left(p_k^{(1)}\right)^2\Theta_k^{(1)}(x,z)\right),$$

$$\sigma_{xz}^{(1)} = \frac{1}{\pi}Re\left(\sum_{k=1}^{6}p_k^{(1)}\Theta_k^{(1)}(x,z)\right),$$

$$\sigma_{zz}^{(1)} = -\frac{1}{\pi} Re\left(\sum_{k=1}^{6} \Theta_k^{(1)}(x,z)\right),$$

$$u_x^{(1)} = -\frac{1}{\pi} Re\left(\sum_{k=1}^{6} \xi_k^{(1)} \Psi_k^{(1)}(x,z)\right),$$

$$u_z^{(1)} = -\frac{1}{\pi} Re\left(\sum_{k=1}^{6} \eta_k^{(1)} \Psi_k^{(1)}(x,z)\right), \tag{51}$$

$$E_x^{(1)} = \frac{1}{\pi} Re\left(\sum_{k=1}^{6} \varsigma_k^{(1)} \Theta_k^{(1)}(x,z)\right),$$

$$E_z^{(1)} = \frac{1}{\pi} Re\left(\sum_{k=1}^{6} \gamma_k^{(1)} \Theta_k^{(1)}(x,z)\right),$$

$$D_x^{(1)} = \frac{1}{\pi} Re\left(\sum_{k=1}^{6} \lambda_k^{(1)} p_k^{(1)} \Theta_k^{(1)}(x,z)\right),$$

$$D_z^{(1)} = -\frac{1}{\pi} Re\left(\sum_{k=1}^{6} \lambda_k^{(1)} \Theta_k^{(1)}(x,z)\right),$$

for material 1, and for material 2,

$$\sigma_{xx}^{(2)} = -\frac{1}{\pi} Re\left(\sum_{k=4}^{6} \left(p_k^{(2)}\right)^2 \Theta_k^{(2)}(x,z)\right),$$

$$\sigma_{xz}^{(2)} = \frac{1}{\pi} Re\left(\sum_{k=4}^{6} p_k^{(2)} \Theta_k^{(2)}(x,z)\right),$$

$$\sigma_{zz}^{(2)} = -\frac{1}{\pi} Re\left(\sum_{k=4}^{6} \Theta_k^{(2)}(x,z)\right),$$

$$u_x^{(2)} = -\frac{1}{\pi} Re\left(\sum_{k=4}^{6} \xi_k^{(2)} \Psi_k^{(2)}(x,z)\right),$$

$$u_z^{(2)} = -\frac{1}{\pi} Re\left(\sum_{k=4}^{6} \eta_k^{(2)} \Psi_k^{(2)}(x,z)\right), \tag{52}$$

$$E_x^{(2)} = \frac{1}{\pi} Re\left(\sum_{k=4}^{6} \varsigma_k^{(2)} \Theta_k^{(2)}(x,z)\right),$$

$$E_z^{(2)} = \frac{1}{\pi} Re\left(\sum_{k=4}^{6} \gamma_k^{(2)} \Theta_k^{(2)}(x,z)\right),$$

$$D_x^{(2)} = \frac{1}{\pi} Re\left(\sum_{k=4}^{6} \lambda_k^{(2)} p_k^{(2)} \Theta_k^{(2)}(x,z)\right),$$

$$D_z^{(2)} = -\frac{1}{\pi} Re\left(\sum_{k=4}^{6} \lambda_k^{(2)} \Theta_k^{(2)}(x,z)\right),$$

where

$$\Theta_s^{(1)}(x,z) = \sum_{n=0}^{\infty} \sum \sum_{l=4}^{6} \sum_{i=1}^{6} \sum_{j=1}^{6} \sum_{k=j+1}^{6} \frac{(-1)^n ivA_{123}^{-1} q_i z_{lijk} \hat{A} G_{sl}}{x + p_s^{(1)} z + \left(\left(p_1^{(1)} + p_2^{(1)} + p_3^{(1)}\right)(n+1) + p_i^{(1)} + p_j^{(1)} + p_k^{(1)} - \hat{P}\right) h - p_i^{(1)} d},$$

$$\Theta_s^{(2)}(x,z) = \sum_{n=0}^{\infty} \sum \sum_{i=1}^{6} \sum_{j=1}^{6} \sum_{k=j+1}^{6} \frac{(-1)^n ivA_{123}^{-1} q_i z_{sijk} \hat{A}}{x + p_s^{(1)} z + \left(\left(p_1^{(1)} + p_2^{(1)} + p_3^{(1)}\right)(n+1) + p_i^{(1)} + p_j^{(1)} + p_k^{(1)} - \hat{P}\right) h - p_i^{(1)} d},$$

$$\Psi_s^{(1)}(x,z) = \sum_{n=0}^{\infty} \sum \sum_{l=4}^{6} \sum_{i=1}^{6} \sum_{j=1}^{6} \sum_{k=j+1}^{6} (-1)^n ivA_{123}^{-1} q_i z_{lijk} G_{sl} \hat{A}$$
$$\ln\left(i\left(x + p_s^{(1)} z + \left(\left(p_1^{(1)} + p_2^{(1)} + p_3^{(1)}\right)(n+1) + p_i^{(1)} + p_j^{(1)} + p_k^{(1)} - \hat{P}\right) h - p_i^{(1)} d\right)\right),$$

$$\Psi_s^{(2)}(x,z) = \sum_{n=0}^{\infty} \sum \sum_{i=1}^{6} \sum_{j=1}^{6} \sum_{k=j+1}^{6} (-1)^n ivA_{123}^{-1} q_i z_{sijk} \hat{A}$$
$$\ln\left(i\left(x + p_s^{(1)} z + \left(\left(p_1^{(1)} + p_2^{(1)} + p_3^{(1)}\right)(n+1) + p_i^{(1)} + p_j^{(1)} + p_k^{(1)} - \hat{P}\right) h - p_i^{(1)} d\right)\right),$$

and $Re[\,]$ denotes the real part. Thus, the first three terms in (51) are fundamental solutions of piezoelectric infinite plane subjected to generalized concentrated forces and edge dislocations. All the remaining terms in (51) and all terms in (52) are image singularities that are induced to satisfy the boundary and interface continuity conditions. Hence, this mathematical method provided in this study is referred to as the generalization method of image.

4 Image Forces Exerted on Edge Dislocations in Piezoelectric Layered Half-plane

The study of dislocations in multilayered structures is important as a means of understanding the mechanical properties of composites and thin films. The motion of a dislocation is related to the image force or the Peach-Koehler (1950) force exerted on the dislocation. The image force that exerts on the dislocation is dependent on the location of the dislocation. The force exerted on the dislocation is most conveniently obtained from Peach-Koehler formula. The solutions of image forces available in the literature have been obtained for relatively simple problems such as isotropic screw or edge dislocations, most of which used multiple image analysis. However, this method is not applicable for the problem of edge dislocations in a multilayered piezoelectric medium.

In this section, our attention will focus on the image forces exerted on edge dislocations in the piezoelectric layered half-plane. The image force can be used to understand the motion of dislocations due to the interaction with the interface boundaries, defects and other dislocations. According to the generalized Peach-Koehler formula, the explicit form of the image force acting on the edge dislocation can be obtained from the stress fields at the location of the edge dislocation minus the self-stresses of the edge dislocation in an infinite medium. The image force exerted on the edge dislocation can be calculated as the summation of force due to the stress fields of all the image singularities in the solution which is provided in the previous section. In Cartesian coordinate, relations between image forces and stress fields are

$$F_x^{(1)} = b_x \hat{\sigma}_{xz}^{(1)},\ F_z^{(1)} = -b_x \hat{\sigma}_{xx}^{(1)}, \tag{53}$$

where $F_x^{(1)}$ and $F_z^{(1)}$ denote image forces exerted on edge dislocation at the thin layer along the horizontal and vertical directions, respectively, and $\hat{\sigma}_{xz}^{(1)} = \sigma_{xz}^{(1)} - \sigma_{xz}^{s}$, $\hat{\sigma}_{xx}^{(1)} = \sigma_{xx}^{(1)} - \sigma_{x}^{s}$ in which $\sigma_{xz}^{(1)}$ and $\sigma_{xx}^{(1)}$ are the stresses given in Eq. (51), σ_{xz}^{s} and σ_{xx}^{s} are the self-stresses of the edge dislocation. The self-stresses of an edge dislocation b_x applied at $(0,d)$ in an infinite piezoelectric medium, which is also presented in the first three terms of Eq. (51), can be written as

$$\sigma_{xz}^{s} = \frac{1}{\pi} Re \sum_{k=1}^{3} \frac{i q_k p_k^{(1)}}{x + p_k^{(1)}(z-d)}\Bigg|_{b_x},\ \sigma_{xx}^{s} = -\frac{1}{\pi} Re \sum_{k=1}^{3} \frac{i q_k \left(p_k^{(1)}\right)^2}{x + p_k^{(1)}(z-d)}\Bigg|_{b_x}. \tag{54}$$

5 Numerical results

Computational programs for numerical calculations of full-field distributions for field variables and image forces are constructed by using the explicit expression of the solutions presented in previous sections. The material properties and characteristic roots for material 1 (PZT-4) are indicated as follows (Rajapakse, 1997; Ding et al., 1999):

$$s_{11}^{(1)} = 10.9 \times 10^{-12}(\mathrm{m^2N^{-1}}), \quad s_{33}^{(1)} = 7.9 \times 10^{-12}(\mathrm{m^2N^{-1}}),$$

$$s_{44}^{(1)} = 19.3 \times 10^{-12}(\mathrm{m^2N^{-1}}), \quad s_{12}^{(1)} = -5.42 \times 10^{-12}(\mathrm{m^2N^{-1}}),$$

$$s_{13}^{(1)} = -2.1 \times 10^{-12}(\mathrm{m^2N^{-1}}),$$

$$g_{15}^{(1)} = -39.4 \times 10^{-3}(\mathrm{m^2C^{-1}}), \quad g_{31}^{(1)} = -11.1 \times 10^{-3}(\mathrm{m^2C^{-1}}),$$

$$g_{33}^{(1)} = 26.1 \times 10^{-3}(\mathrm{m^2C^{-1}}),$$

$$\beta_{11}^{(1)} = 7.94 \times 10^{7}(\mathrm{m^2NC^{-2}}), \quad \beta_{33}^{(1)} = 9.02 \times 10^{7}(\mathrm{m^2NC^{-2}}),$$

$$p_1^{(1)} = 1.2038i, \quad p_2^{(1)} = 0.2004 + 1.0691i, \quad p_3^{(1)} = -0.2004 + 1.0691i.$$

For material 2, the material properties and characteristic roots of PZT-7A (Li et al., 2003) are given below:

$$s_{11}^{(2)} = 9.7 \times 10^{-12}(\mathrm{m^2N^{-1}}), \quad s_{33}^{(2)} = 7.85 \times 10^{-12}(\mathrm{m^2N^{-1}}),$$

$$s_{44}^{(2)} = 21.8 \times 10^{-12}(\mathrm{m^2N^{-1}}),$$

$$s_{12}^{(2)} = -4.2 \times 10^{-12}(\mathrm{m^2N^{-1}}), \quad s_{13}^{(2)} = -2.3 \times 10^{-12}(\mathrm{m^2N^{-1}}),$$

$$g_{15}^{(2)} = 48.8 \times 10^{-3}(\mathrm{m^2C^{-1}}), \quad g_{31}^{(2)} = -15.9 \times 10^{-3}(\mathrm{m^2C^{-1}}),$$

$$g_{33}^{(2)} = 39.3 \times 10^{-3}(\mathrm{m^2C^{-1}}),$$

$$\beta_{11}^{(2)} = 13.48 \times 10^{7}(\mathrm{m^2NC^{-2}}), \quad \beta_{33}^{(2)} = 26.50 \times 10^{7}(\mathrm{m^2NC^{-2}}),$$

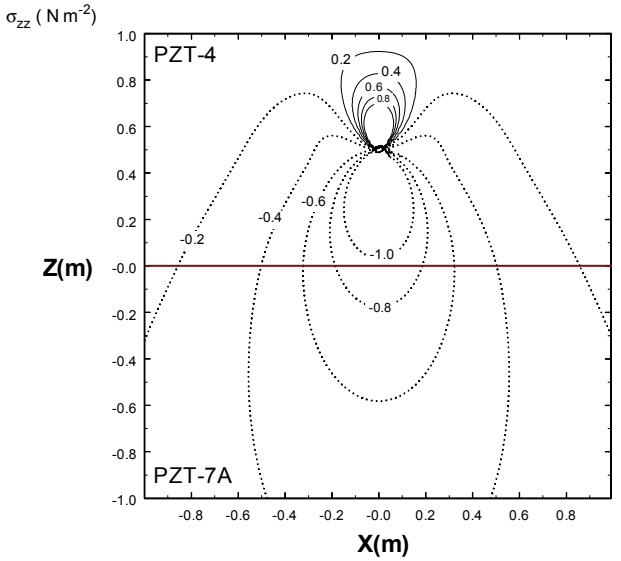

Figure 2: Full-field distribution of normal stress σ_{zz} for the piezoelectric layered half-plane subjected to a concentrated force f_z in the layer for $d = 0.5h$.

$$p_1^{(2)} = 1.6719i, \quad p_2^{(2)} = 1.1591i, \quad p_3^{(2)} = 0.8967i.$$

A more comprehensive investigation of the piezoelectric layered half-plane can be made by plotting full-field distribution contours of the field variables. In full-field distribution contours, short dash lines and solid lines indicate negative and positive values, respectively. Figs. 2, 3 and 4 show the contours of stresses σ_{zz}, σ_{xz} and σ_{xx}, respectively, for the layered half-plane subjected to a line force f_z with magnitude -1 Nm^{-1} applied at $(x,z) = (0,0.5)$ in the thin layer (material 1). These figures indicate that the full-field distributions of σ_{xz} and σ_{zz} are continuous at the interface and are zero on the free surface. The symmetric contours for σ_{zz} and σ_{xx} with respect to the z-axis is due to the transversely isotropic constitutive properties of the materials. In addition, the contour of stress σ_{xz} is zero along the z-axis due to the anti-symmetric nature of the solutions. Figs. 5 and 6 represent the contours of electric fields E_x and E_z for a line force f_z with magnitude -1 Nm^{-1} applied at $(x,z) = (0,0.5)$ in material 1, respectively.

In order to discuss the influence of the material constants on image forces of edge dislocations, two more piezoelectric materials are used in the analysis, which in-

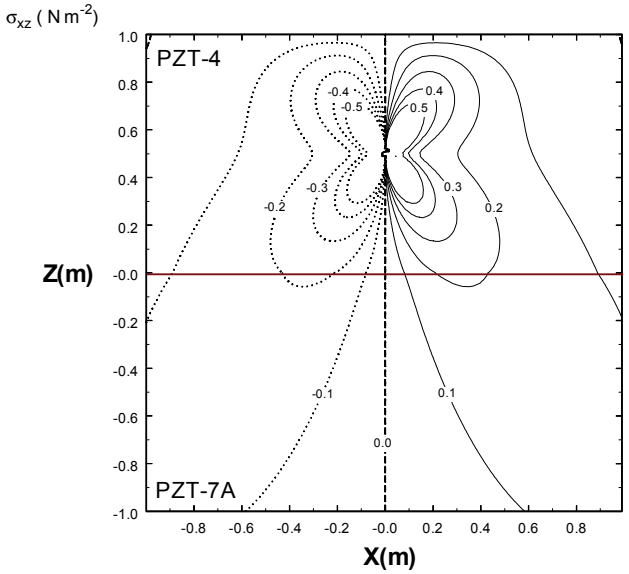

Figure 3: Full-field distribution of shear stress σ_{xz} for the piezoelectric layered half-plane subjected to a concentrated force f_z in the layer for $d = 0.5h$.

cludes PZT-5A and PZT-5H. The material properties for PZT-5A are indicated as follows.

$$s_{11} = 14.4 \times 10^{-12}(\mathrm{m^2N^{-1}}), \quad s_{33} = 9.46 \times 10^{-12}(\mathrm{m^2N^{-1}}),$$
$$s_{44} = 25.2 \times 10^{-12}(\mathrm{m^2N^{-1}}),$$

$$s_{12} = -7.71 \times 10^{-12}(\mathrm{m^2N^{-1}}), \quad s_{13} = -2.98 \times 10^{-12}(\mathrm{m^2N^{-1}}),$$

$$g_{15} = 38.2 \times 10^{-3}(\mathrm{m^2C^{-1}}), \quad g_{31} = -11.4 \times 10^{-3}(\mathrm{m^2C^{-1}}),$$
$$g_{33} = 24.8 \times 10^{-3}(\mathrm{m^2C^{-1}}),$$

$$\beta_{11} = 6.54 \times 10^{7}(\mathrm{m^2NC^{-2}}), \quad \beta_{33} = 6.66 \times 10^{7}(\mathrm{m^2NC^{-2}}).$$

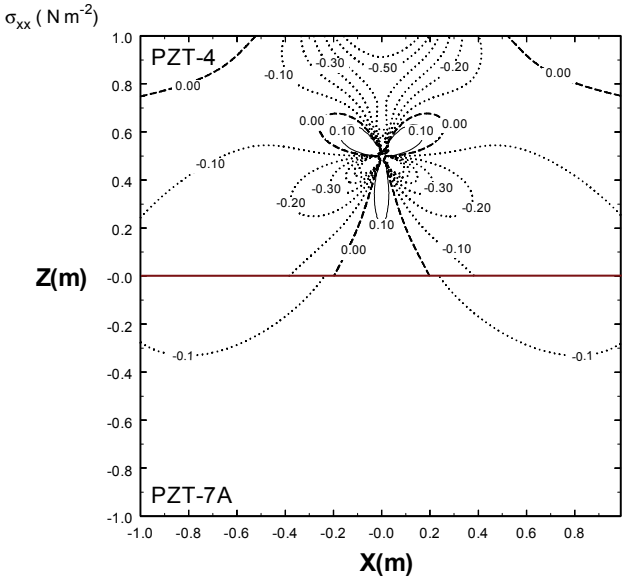

Figure 4: Full-field distribution of normal stress σ_{xx} for the piezoelectric layered half-plane subjected to a concentrated force f_z in the layer for $d = 0.5h$.

The material properties of PZT-5H are given below:

$$s_{11} = 14. \times 10^{-12}(\mathrm{m^2N^{-1}}), \quad s_{33} = 9.05 \times 10^{-12}(\mathrm{m^2N^{-1}}),$$

$$s_{44} = 23.7 \times 10^{-12}(\mathrm{m^2N^{-1}}),$$

$$s_{12} = -7.27 \times 10^{-12}(\mathrm{m^2N^{-1}}), \quad s_{13} = -3.05 \times 10^{-12}(\mathrm{m^2N^{-1}}),$$

$$g_{15} = 26.8 \times 10^{-3}(\mathrm{m^2C^{-1}}), \quad g_{31} = -9.11 \times 10^{-3}(\mathrm{m^2C^{-1}}),$$

$$g_{33} = 19.7 \times 10^{-3}(\mathrm{m^2C^{-1}}),$$

$$\beta_{11} = 3.61 \times 10^{7}(\mathrm{m^2NC^{-2}}), \quad \beta_{33} = 3.32 \times 10^{7}(\mathrm{m^2NC^{-2}}).$$

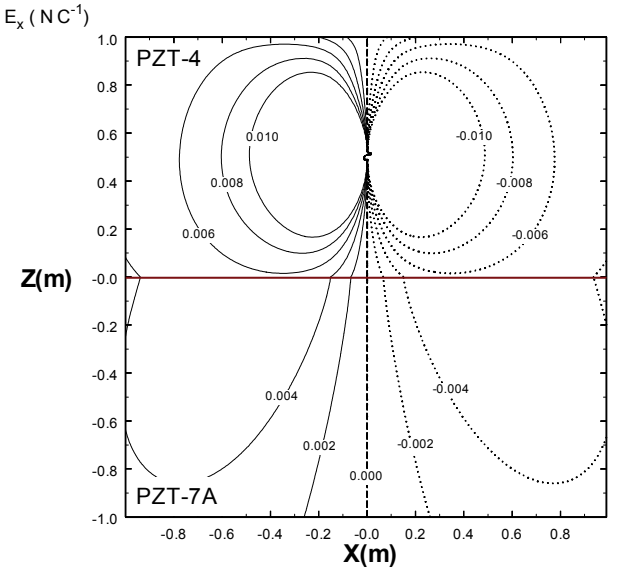

Figure 5: Full-field distribution of electric field E_x for the piezoelectric layered half-plane subjected to a concentrated force f_z in the layer for $d = 0.5h$.

The image forces exerted on an edge dislocation b_x in the piezoelectric layered half-plane for different material combinations are shown in Fig. 7. The locations of equilibrium points depend on material constants. It is clearly observed from Fig. 7 that the image force exerted on the edge dislocation is positive near the free surface, and therefore the free surface always attracts the edge dislocation. In addition, the image force near the interface in the layer for all the cases in Fig. 7 is negative; hence the interface always attracts the edge dislocation. Hence there is an unstable equilibrium point (i.e.,$F_z^{(1)} = 0$) in the layer for all the cases. It is also indicated in Fig. 7 that the location of the equilibrium point is always near the interface.

6 Conclusions

This study provides a complete investigation of the two-dimensional planar problem of elastic and electric fields induced by generalized line forces and edge dislocations applied in a transversely isotropic piezoelectric layered half-plane. By using Fourier-transform method and the series expansion technique, the analytical full-field solutions for the displacements, stresses, electrical displacements, and electric fields are presented in explicit forms. The complete solutions for this prob-

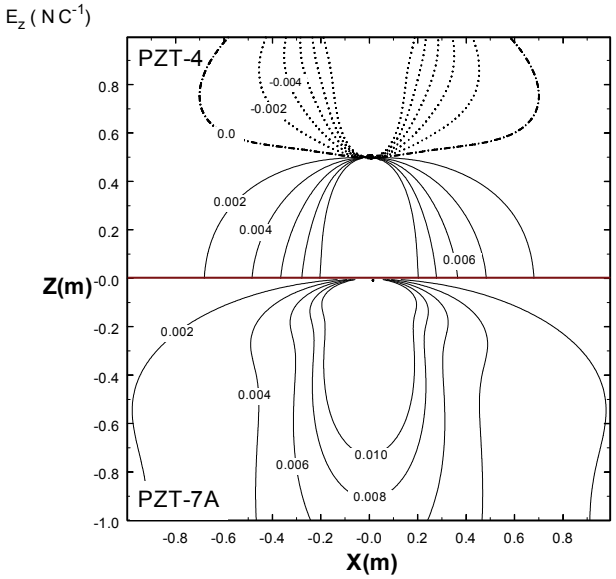

Figure 6: Full-field distribution of magnetic field E_z for the piezoelectric layered half-plane subjected to a concentrated force f_z in the layer for $d = 0.5h$.

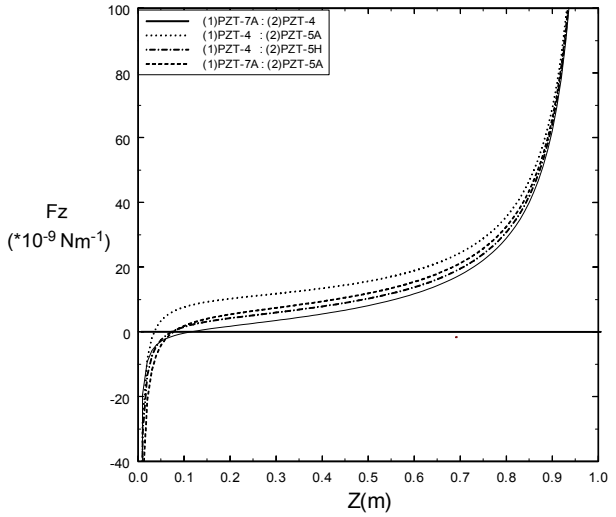

Figure 7: Distribution of the image forces F_z exerted on an edge dislocation b_x with different material combinations.

lem consist only the simplest solutions of an infinite piezoelectric medium with applied loadings. Except the solution for the originally applied loading in an infinite medium, the other image singularities are induced to satisfy the free surface and interface continuity conditions. Therefore, the physical meaning of the analytical solution is regarded as the generalized image method. The mathematical approach used in this study provides an automatic determination of the locations and magnitudes of all the image singularities. It is also shown that the locations and magnitudes of image singularities are dependent on the characteristic roots of the layered half-plane. The explicit full-field solutions are used to construct the image forces for one edge dislocation. Computational programs for numerical calculations of the full-field distribution of stresses, electric fields and image forces exerted on an edge dislocation can be easily constructed by using the explicit formulation of the analytical solutions.

Acknowledgement: This paper is dedicated to Professor Wen-Hwa Chen on the occasion of his 60th birthday and also on his contributions for the computational solid mechanics and fracture mechanics. The authors gratefully acknowledge Grant NSC 94-2212-E002-018 from the National Science Council (Republic of China) to National Taiwan University.

References

Barnett, D.M.; Lothe, J. (1974): An image force theorem for dislocations in anisotropic bicrystals. *J. Phys. F: Met. Phys.*, vol. 4, pp. 1618-1635.

Chen, B.J.; Xiao, Z.M.; Liew, K.M. (2004): A line dislocation interacting with a semi-infinite crack in piezoelectric solid. *Int. J. Solids Struct.*, vol. 42, pp. 1-11.

Chen, K.H.; Kao, J.H.; Chen, J.T. (2009): Regularized meshless method for antiplane piezoelectricity problems with multiple inclusions. *CMC: Computers, Materials & Continua*, vol. 9, pp. 253-279.

Ding, H.; Chi, Y.; Guo, F. (1999): Solutions for transversely isotropic piezoelectric infinite body, semi-infinite body and bimaterial infinite body subjected to uniform ring loading and charge. *Int. J. Solids Struct.*, vol. 36, pp. 2613-2631.

Eshelby, J.D.; Read, W.T.; Shockley, W. (1953): Anisotropic elasticity with applications to dislocation theory. *Acta Metall.*, vol. 1, pp. 251-259.

Huang, Z.; Kuang, Z.B. (2001): Dislocation inside a piezoelectric media with an elliptic inhomogeneity. *Int. J. Solids Struct.*, vol. 38, pp. 8459-8479.

Lee, J.M.; Ma, C.C. (2007): Analytical full-field solutions of a magnetoelectroelastic layered half-plane. *J. Appl. Phys.*, vol. 101, 083502.

Li, Z.; Wang, C.; Chen, C. (2003): Effective electromechanical properties of transversely isotropic piezoelectric ceramics with microvoids. *Compu. Mater. Sci.*, vol. 27, pp. 381-392.

Lin, R.L.; Ma, C.C. (2000): Antiplane deformations for anisotropic multilayered media by using the coordinate transform method. *J. Appl. Mech. ASME*, vol. 67, pp. 597-605.

Liu, J.X.; Wang, X.Q. (2004): Interaction of a screw dislocation with a notch in a piezoelectric bi-material. *Arch. Appl. Mech.*, vol. 73, pp. 553-560.

Ma, C.C.; Lee, J.M. (2007): Image forces of screw dislocations in a magnetoelectroelastic layered half-plane. *J. Appl. Phys.*, vol. 101, 123513.

Ma, C.C.; Lin, R.L. (2001): Image singularities of Green's functions for an isotropic elastic half-plane subjected to forces and dislocations. *Math. Mech. Solids*, vol. 6, pp. 503-524.

Ma, C.C.; Lin, R.L. (2002): Image singularities of Green's functions for isotropic elastic bimaterials subjected to forces and dislocations. *Int. J. Solids Struct.*, vol. 39, pp. 5253-5277.

Ma, C.C.; Lu, H.T. (2006): Theoretical analysis of screw dislocations and image forces in anisotropic multilayered media. *Phys. Rev. B*, vol. 73, 144102.

Ma, C.C.; Wu, K.C.; Lee, J.M. (2008): Full-field analysis and image forces for piezoelectric bimaterials. *Acta Mech.*, vol. 195, pp. 275-294.

Pak, Y.E. (1990): Force on a piezoelectric screw dislocation. *J. Appl. Mech. ASME*, vol. 57, pp. 863-869.

Peach, M.D.; Koehler, J.S. (1950): The force exerted on dislocations and the stress field produced by them. *Phys. Rev.*, vol. 80, pp. 436-439.

Rajapakse, R.K.N.D. (1997): Plane strain/plane stress solutions for piezoelectric solids. *Composites Part B*, vol. 28, pp. 385-396.

Sosa, H. (1991): Plane problems in piezoelectric media with defects. *Int. J. Solids Struct.*, vol. 28, pp. 491-505.

Stroh, A.N. (1958): Dislocations and cracks in anisotropic elasticity. *Philos. Mag,.,* vol. 7, pp. 625-646.

Ting, T. C. T. (1996): Anisotropic Elasticity. Oxford University Press, New York, USA.

Ting, T.C.T.; Barnett, D.M. (1993): Image force on line dislocations in anisotropic elastic half-spaces with a fixed boundary. *Int. J. Solids Struct.*, vol. 30, pp. 313-323.

Wang, X.; Sudak, L. (2007): A piezoelectric screw dislocation interacting with

an imperfect piezoelectric bimaterial interface. *Int. J. Solids Struct.*, vol. 44, pp. 3344-3358.

Willis, J.R. (1970): Stress field produced by dislocations in anisotropic media. *Philos. Mag.*, vol. 21, pp. 931-949.

Wu, C.P.; Chiu, K.H.; Wang, Y.M. (2008): A review on the three-dimensional analytical approaches of multilayered and functionally graded piezoelectric plates and shells. *CMC: Computers, Materials & Continua*, vol. 8, pp. 93-132.

Wu, X.F.; Cohn, S.; Dzenis, Y.A. (2003): Screw dislocation interacting with interfacial and interface cracks in piezoelectric bimaterials. *Int. J. Solids Struct.*, vol. 41, pp. 667-682.